Received November 29, 2019, accepted December 12, 2019, date of publication December 17, 2019, date of current version December 31, 2019.

Digital Object Identifier 10.1109/ACCESS.2019.2960397

Variable Impulsive Synchronization of Memristor-Based Chaotic Systems With Actuator Saturation

ZHILI XIONG [1,2], ZHENGLE ZHANG [3,4], AND TIEDONG MA [3,4], (Member, IEEE)
[1]Department of Electronics and Information Engineering, Central China Normal University, Wuhan 430079, China
[2]Department of Physics and Electric Information, Huanggang Normal University, Huanggang 438000, China
[3]Key Laboratory of Complex System Safety and Control (Chongqing University), Ministry of Education, Chongqing 400044, China
[4]School of Automation, Chongqing University, Chongqing 400044, China

Corresponding author: Tiedong Ma (tdma@cqu.edu.cn)

This work was supported in part by the Fundamental Research Funds for the Central Universities under Grant 2019CDXYZDH0014, Grant 2019CDYGZD010, Grant 2019CDCGZDH207, and Grant 2019CDCGZDH211, in part by the National Natural Science Foundation of China under Grant 61673078, in part by the Basic and Frontier Research Project of Chongqing under Grant cstc2019jcyj-msxmX0418, and in part by the Graduate Scientific Research and Innovation Foundation of Chongqing, China, under Grant CYS19018.

ABSTRACT This paper is concerned with the synchronization of memristor-based chaotic system subject to actuator saturation via variable impulsive control. Firstly, a memristor-based circuit model is considered, and an impulsive controller subject to actuator saturation is designed. Based on the Lyapunov stability theory and some inequality techniques, some sufficient conditions are derived to guarantee the asymptotic synchronization of the memristor-based chaotic systems. Compared with the common fixed impulsive control, the variable impulsive control used in this paper is more reliable in practical application. Finally, the numerical simulations are given to verify the effectiveness of the proposed method.

INDEX TERMS Synchronization, memristor-based chaotic system, variable impulsive control, actuator saturation.

I. INTRODUCTION

The memristor was first postulated as the fourth circuit component by Leon O. Chua in 1971 [1]. It replaces other more familiar circuit elements, such as resistors, capacitors and inductors. However, until a team of scientists at HP Labs announced that they had built a prototype memristor in 2008, the great discovery did not attract scientists' attention [2]. Since then, it has been widely studied in theory and application. Itoh and Chua as well as Muthuswamy and Kokate proposed some memristor-based circuits [3], [4]. In the last five years, memristor-based system has been widely studied by many scholars [5]–[12]. Reference [5] studied a kind of inertia neural network (Minn) based on memristor with external input and output. Reference [6] used nonsmooth analysis and control theory to deal with chaotic neural network based on memristor with discontinuous right hand side. In [7], a new neural network with time-varying delay based on complex memristor was proposed and its exponential stability was discussed. A novel memristor chaotic circuit was proposed in [8], which was derived from classical Chua's circuit by replacing Chua's diode with a first-order memristor diode bridge. In [9], a novel Chua's hyperchaotic circuit based on five-order dual memristors was introduced. In [10], a control strategy for extreme multistability exhibited in an active band pass filter-based memristive circuit was explored in flux–charge domain. Reference [11] investigated extreme multistability and its controllability for an ideal voltage-controlled memristor emulator-based canonical Chua's circuit. Some unrevealed features of a newly introduced megastable chaotic oscillator was investigated in [12], and a novel fuzzy-based robust and adaptive control method was designed to control this oscillator. In [13], two ideal memristor simulators and the fifth order memristor Chua's circuit based on them were analyzed from a new perspective of flux and charge.

In recent years, the synchronization problem of chaotic systems has attracted extensive attention [14]–[18]. So far, many different methods have been proposed to solve the synchronization problem of memristor-based chaotic systems, such as pinning control [19], adaptive control [20], sliding mode control [21], finite-time control [22], etc. Compared with continuous control method, the impulsive control method based on impulsive differential equation can reduce the state information transmission load greatly, where the state information between the master and slave chaotic systems is transmitted only at impulsive instants. It is obviously

The associate editor coordinating the review of this manuscript and approving it for publication was Rajeeb Dey.

that the impulsive control method has high robustness and low control cost in practical applications [23]–[25].

In the actual control system, the controller mostly drives the controlled object through the actuator. Due to the physical limitation of the actuator, the control input cannot be arbitrarily large. On the other hand, if the actuator saturation is not considered in the designing of control system, the system performance will be deteriorated, such as causing hysteresis, overshoot, increase of adjustment time, increased oscillation, etc., and even lead to system instability [26]–[28]. Because of the importance of saturation, there have been many achievements on actuator saturation of chaotic systems in recent years [29]–[31]. For example, the synchronization of chaotic systems with unknown control direction subject to input saturation nonlinearity was studied in [29]. In [30], the stabilization of actuators saturation in uncertain chaotic systems was investigated by an adaptive PID control method. The prescribed performance adaptive neural network synchronization was researched for a class of unknown chaotic systems subject to input saturation in [31]. However, there are few works about the actuator saturation of memristor-based chaotic circuits. For example, Reference [32] investigated the H_∞ control design for memristor-based neural networks (MNNs) in the presence of actuator saturation and external disturbance. Note that the above literatures adopted the continuous control methods. Due to the high robustness and low control cost of the impulsive control, it is necessary to explore the synchronization problem of master-slave memristor-based systems.

In the literature on impulsive synchronization of chaotic systems with master and slave memristors, some important issues have been investigated, such as time-delayed in memristor-based chaotic systems [33], TS fuzzy model [34], pinning impulsive control [35], finite-time synchronization [36], etc. It should be noted that the impulsive control schemes proposed in the above literatures were carried out at fixed impulsive instants. However, in practical applications, due to hardware constraints and disturbance, the system cannot accurately be imposed at the expected impulsive instants, and there will be deviation between the expected instants and the actual occurrence instants [37]–[39]. For example, we plan to input an control impulse at time instant η, But the actuator might place the impulse in a time window $[\eta - \upsilon, \eta + \upsilon]$, where η and υ are the center and radius of the impulsive time window respectively. This situation obviously does not meet the theoretical synchronization conditions of fixed impulsive control, thus it is important to study the synchronization of memristor-based chaotic systems with variable impulsive control. In recent years, there are many literatures about variable impulsive control, such as stochastic fuzzy delayed neural networks [40], cyclic control system [41], sandwich control systems [42], a class of stochastic systems [43], periodically control system [44], a memristor-based lorenz circuit [45], memristor-based chaotic system [46].

Inspired by the above discussions, the purpose of this paper is to study the variable impulsive synchronization of master and slave memristor-based chaotic system subject to actuator saturation. By designing an effective variable impulsive controller, some sufficient conditions are obtained. The synchronization of memristor-based system with actuator saturation can be realized, which is more effective in practical application. As far as we know, there is little work to combine variable control method with actuator saturation of memristor-based chaotic system. It is noteworthy that this paper adopts two types of impulsive time window methods: left endpoint and center point. Compared with the existing fixed impulsive control algorithms, the variable impulsive control method adopted in this paper can allow the error at a certain impulse input instants. Therefore, the synchronization scheme with variable impulsive control and actuator saturation is more practical in actual application.

The remainder of this paper is arranged as follows. In Section 2, the model of master and slave memristor-based chaotic systems is given. In Section 3, variable impulsive synchronization of master and slave memristor-based chaotic systems subject to actuator saturation is analyzed. In Section 4, the effectiveness of the main results is verified by the numerical simulation examples. Finally, the conclusion of this paper is drawn in Section 5.

Throughout this paper, $\mathbb{R}$, $\mathbb{R}^n$, $\mathbb{R}^{m\times n}$ denote the real numbers, the n-dimensional Euclidean space, the set of all $m \times n$ real matrices respectively. $\lambda_{\max}(\Upsilon)$ denotes the maximal eigenvalue of matrix Υ. Let $\mathbb{N} = \{1, 2, ...\}$. I_n is the n dimensional identity matrix. $\otimes$ denote the Kronecker product, $\mathrm{diag}\{d_1, \ldots, d_n\}$ denotes the diagonal matrix with diagonal elements d_1 to d_n.

II. PROBLEM DESCRIPTION

The memristor-based chaotic circuit considered in this paper was described in [47], [48], which is shown in Fig.1.

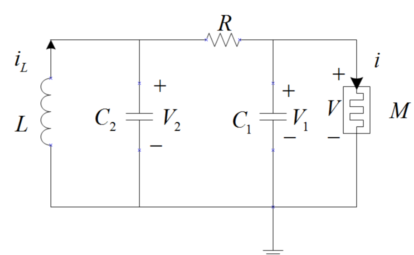

FIGURE 1. The memristor-based chaotic circuit.

From Fig.1, the memristor-based chaotic system can be written as follows:

$$\begin{cases} \dfrac{dv_1(t)}{dt} = \dfrac{1}{C_1}\left(\dfrac{v_2(t) - v_1(t)}{R} - i(t)\right), \\ \dfrac{dv_2(t)}{dt} = \dfrac{1}{C_2}\left(\dfrac{v_1(t) - v_2(t)}{R} - i_L(t)\right), \\ \dfrac{di_L(t)}{dt} = \dfrac{v_2(t)}{L}, \\ \dfrac{d\varphi}{dt} = v_1(t), \end{cases} \tag{1}$$

where φ is flux, $i(t)$ is derived in [49],

$$i(t) = W(\varphi)v_1(t) = \frac{dq}{d\varphi}v_1(t), \tag{2}$$

where q is charge, $W(\varphi) = dq/d\varphi = \alpha + 3\beta\varphi^2$ is the flux-dependent rate of change of charge.

In order to obtain the chaos generation, the parameters of (1) generating chaotic dynamics are as follows: $R = 2\text{k}\Omega, L = 15.8mH, C_1 = 6.1\mu F, C_2 = 71\mu F$, $\alpha = -0.663 * 10^{-3}$ and $\beta = 0.004 * 10^{-3}$.

For convenience, let $v_1 = x_1, v_2 = x_2, i_L = x_3$, $\varphi = x_4$; $a_1 = 1/C_1, a_2 = 1/C_2, a_3 = 1/R, a_4 = 1/L$, then the memristor-based chaotic system is given as

$$\begin{cases} \dot{x}_1 = a_1(a_3(x_2 - x_1) - W(x_4)x_1), \\ \dot{x}_2 = a_2(a_3(x_1 - x_2) - x_3), \\ \dot{x}_3 = a_4 x_2, \\ \dot{x}_4 = x_1, \end{cases} \tag{3}$$

which is equivalent to

$$\begin{cases} \dot{x}_1 = a_1(a_3(x_2 - x_1) - \alpha x_1 - 3\beta x_1 x_4^2), \\ \dot{x}_2 = a_2(a_3(x_1 - x_2) - x_3), \\ \dot{x}_3 = a_4 x_2, \\ \dot{x}_4 = x_1. \end{cases} \tag{4}$$

The memristor-based chaotic circuit system in (3) can be decomposed into linear and nonlinear parts, so one can rewrite it as

$$\dot{x} = Ax + \psi(x), \tag{5}$$

where

$$x = [x_1, x_2, x_3, x_4]^T,$$
$$A = \begin{bmatrix} -a_1(\alpha + a_3) & a_1 a_3 & 0 & 0 \\ a_2 a_3 & -a_2 a_3 & -a_2 & 0 \\ 0 & a_4 & 0 & 0 \\ 1 & 0 & 0 & 0 \end{bmatrix},$$
$$\psi(x) = \begin{bmatrix} -3a_1\beta x_1 x_4^2 \\ 0 \\ 0 \\ 0 \end{bmatrix}.$$

Let system (5) be the master memristor-based chaotic circuit system, and the slave system is given as

$$\dot{y} = Ay + \psi(y), \tag{6}$$

where $y = [y_1, y_2, y_3, y_4]^T$ is the state variables of the driven system, and the synchronization error vector is defined as $e(t) = y(t) - x(t) = [e_1(t), e_2(t), e_3(t), e_4(t)]^T$.

The controller $u(t) = [u_1(t), u_2(t), u_3(t), u_4(t)]^T$ in (3) is given as

$$u(t) = \text{sat}(B_k e(t_k))\delta(t - t_k), \tag{7}$$

where the impulsive sequence $\{t_k\}$ satisfies $0 < t_0 < t_1 < t_2 < \cdots < t_{k-1} < t_k < \cdots, \lim_{k\to\infty} t_k = \infty$, $\lim_{h\to 0^+} x(t_k + h) = x(t_k^+), \lim_{h\to 0^+} x(t_k - h) = x(t_k^-) = x(t_k)$ implies that $x(t)$ is left continuous at t_k, $\delta(t)$ is the Dirac delta function and satisfies $\delta(t) = 0$ for $t \neq 0$, the saturation function $\text{sat}(B_k e(t_k)) = (\text{sat}(b_{1k}e_1(t_k)), \ldots, \text{sat}(b_{4k}e_4(t_k)))^T$ with $\text{sat}(s) = sign(s)\min\{\Delta, |s|\}, s \in \mathbb{R}$, where $\Delta \in \mathbb{R}^+$ is the known saturation level, $B_k = \text{diag}\{b_{1k}, \ldots, b_{4k}\}$ is the impulsive control gain matrix.

Subtract system (5) from (6), one gets the impulsive synchronization error system

$$\begin{cases} \dot{e} = Ae + \psi(e), \quad t \neq t_k, \\ \Delta e(t_k) = e(t_k^+) - e(t_k^-) = sat(B_k e(t_k)), \quad k \in \mathbb{N}, \end{cases} \tag{8}$$

where $\psi(e) = \psi(y) - \psi(x) = \begin{bmatrix} -3a_1\beta(y_1 y_4^2 - x_1 x_4^2) \\ 0 \\ 0 \\ 0 \end{bmatrix}$.

Define a time-varying parameter $h_i(t_k)$, $i = \{1, 2, 3, 4\}$ as

$$h_i(t_k) = \begin{cases} \dfrac{\Delta}{|b_{ik}e_i(t_k)|} & |b_{ik}e_i(t_k)| > \Delta, \\ 1 & |b_{ik}e_i(t_k)| \le \Delta. \end{cases} \tag{9}$$

It is easy to check that $h_i(t_k) \in (0, 1]$ and the saturation input in (7) can be expressed as

$$\text{sat}(b_{ik}e_i(t_k)) = b_{ik}h_i(t_k)e_i(t_k). \tag{10}$$

Then one can get

$$\begin{aligned} \text{sat}(B_k e(t_k)) &= (\text{sat}(b_{1k}e_1(t_k)), \text{sat}(b_{2k}e_2(t_k)), \\ &\quad \text{sat}(b_{3k}e_3(t_k)), \text{sat}(b_{4k}e_4(t_k)))^T \\ &= (b_{1k}h_1(t_k)e_1(t_k), b_{2k}h_2(t_k)e_2(t_k), \\ &\quad b_{3k}h_3(t_k)e_3(t_k), b_{4k}h_4(t_k)e_4(t_k))^T \\ &= B_k H(t_k)e(t_k), \end{aligned} \tag{11}$$

where $H(t_k) = \text{diag}\{h_1(t_k), h_2(t_k), h_3(t_k), h_4(t_k)\}$.

In this paper, the impulsive controller is designed to synchronize the slave system with the master system, i.e.,

$$\lim_{t\to\infty} e(t) = 0. \tag{12}$$

For convenience and simplicity, all time-varying variables in the rest of this paper will be represented without the time parameter $x \triangleq x(t), y \triangleq y(t), e \triangleq e(t)$.

III. MAIN RESULTS

The relationship between the impulsive radius $\{r_k\}$ and the impulsive centers $\{\tau_k\}$ satisfies assumption 1, and some important moments are shown in Fig. 2. The shaded area in Fig. 2 represents the possible range of the actual pulse time corresponding to the so-called pulse time window.

Assumption 1:

$$\begin{aligned} \tau_{k-1}^l < t_{k-1} < \tau_{k-1}^r < \tau_k^l < t_k < \tau_k^r < \tau_{k+1}^l < t_{k+1} \\ < \tau_{k+1}^r, \quad k \in \mathbb{N}, \end{aligned}$$

where $\tau_k^l = \tau_k - r_k$ and $\tau_k^r = \tau_k + r_k$ are the left and right endpoints of the k-th impulsive time window respectively. τ_k and r_k are the center and radius of the k-th time window.

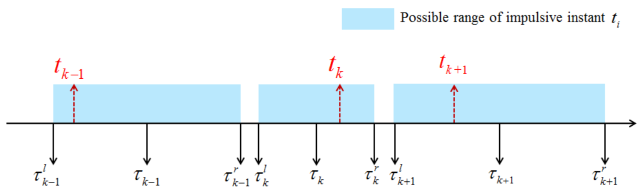

FIGURE 2. **The diagram of impulsive time window.**

Theorem 1: Let Ω denote the chaos attractor of (3) and $|x_1| \le M_1$, $|x_4| \le M_2$, $|y_4| \le M_2$. Let λ_k be the largest eigenvalue of $(I_n + B_k H(t_k))^T (I_n + B_k H(t_k))$, and λ_A be the largest eigenvalue of $A + A^T$. There exists the constant ε and $\xi > 1$ such that

$$(\lambda_A + 6a_1\beta M_1 M_2)(\tau^l_{k+2} - \tau^l_{k+1}) + \ln(\lambda_k \xi) < 0, \quad (13)$$

then the synchronization of memristor-based chaotic circuit system (5) and (6) can be realized with controller (7).

Proof: Choose the Lyapunov function as $V(t) = e^T e$, for $t \in (t_{k-1}, t_k]$,

$$\begin{aligned} D^+V(t) &= \dot{e}^T e + e^T \dot{e} \\ &= e^T (A + A^T)e + e^T \psi(e) + \psi^T(e)e. \\ &\le \lambda_A e^T e - 6a_1\beta(y_1 y_4^2 - x_1 x_4^2)e_1 \\ &= \lambda_A e^T e - 6a_1\beta(y_1 y_4^2 - x_1 y_4^2 + x_1 y_4^2 - x_1 x_4^2)e_1 \\ &= \lambda_A e^T e - 6a_1\beta y_4^2 e_1^2 - 6\alpha_1\beta(x_4^2 - y_4^2)x_1 e_1 \\ &\le \lambda_A e^T e + 3a_1\beta\, |x_1|\, (|x_4| + |y_4|)(e_1^2 + e_4^2) \\ &\le (\lambda_A + 6a_1\beta M_1 M_2)e^T e. \end{aligned} \quad (14)$$

Then (14) can be transformed into

$$D^+V(t) \le (\lambda_A + 6a_1\beta M_1 M_2)V(t). \quad (15)$$

This lead to

$$V(t) \le V((t^+_{k-1}) \exp((\lambda_A + 6a_1\beta M_1 M_2)(t - t_{k-1})). \quad (16)$$

When $t = t_k$, one can get

$$\begin{aligned} V(t^+_k) &= e^T(t^+_k)e(t^+_k) \\ &= e^T(t_k)((B_k H(t_k) + I_n)^T (B_k H(t_k) + I_n))e(t_k) \\ &\le \lambda_k V(t_k). \end{aligned} \quad (17)$$

For $t \in (t_0, \tau^l_1]$, it follows from (16) that

$$V(t) \le V(t_0) \exp((\lambda_A + 6a_1\beta M_1 M_2)(t - t_0)). \quad (18)$$

If $t \in (\tau^l_1, t_1]$, from (16), one can get

$$V(t) \le V(t_0) \exp((\lambda_A + 6a_1\beta M_1 M_2)(t - t_0)). \quad (19)$$

If $t \in (t_1, \tau^l_2]$, from (16) and (17), it yields

$$\begin{aligned} V(t) &\le V(t^+_1) \exp((\lambda_A + 6a_1\beta M_1 M_2)(t - t_1)) \\ &\le \lambda_1 V(t_1) \exp((\lambda_A + 6a_1\beta M_1 M_2)(t - t_1)) \\ &\le \lambda_1 V(t_0) \exp((\lambda_A + 6a_1\beta M_1 M_2)(t - t_0)). \end{aligned} \quad (20)$$

Therefore, for $t \in (\tau^l_1, \tau^l_2]$, one can derive

$$V(t) \le \lambda_1^{\kappa_1} V(t_0) \exp((\lambda_A + 6a_1\beta M_1 M_2)(t - t_0)), \quad (21)$$

where $\kappa_k = \begin{cases} 0, t \le t_k \\ 1, t > t_k \end{cases}, k \in \mathbb{N}$.

In general, for $t \in (\tau^l_{k+1}, \tau^l_{k+2}]$, one can attain

$$\begin{aligned} V(t) &\le V(t_0)\lambda_1\lambda_2 \cdots \lambda_{k-1}\lambda_k\lambda_{k+1}^{\kappa_{k+1}} \\ &\quad \times \exp((\lambda_A + 6a_1\beta M_1 M_2)(t - t_0)) \\ &\le V(t_0)\lambda_1\lambda_2 \cdots \lambda_{k-1}\lambda_k\lambda_{k+1}^{\kappa_{k+1}} \\ &\quad \times \exp((\lambda_A + 6a_1\beta M_1 M_2)(\tau^l_{k+2} - t_0)) \\ &\le V(t_0)\lambda_1 \exp((\lambda_A + 6a_1\beta M_1 M_2)(\tau^l_3 - \tau^l_2)) \\ &\quad \times \lambda_2 \exp((\lambda_A + 6a_1\beta M_1 M_2)(\tau^l_4 - \tau^l_3)) \cdots \\ &\quad \lambda_{k-1} \exp((\lambda_A + 6a_1\beta M_1 M_2)(\tau^l_{k+1} - \tau^l_k)) \\ &\quad \times \lambda_k \exp((\lambda_A + 6a_1\beta M_1 M_2)(\tau^l_{k+2} - \tau^l_{k-1})) \\ &\quad \times \lambda_{k+1}^{\kappa_{k+1}} \exp((\lambda_A + 6a_1\beta M_1 M_2)(\tau^l_2 - \tau_0)). \end{aligned} \quad (22)$$

From condition (13), one can get

$$\lambda_k \exp(\lambda_A + 6a_1\beta M_1 M_2)(\tau^l_{k+2} - \tau^l_{k+1}) < \frac{1}{\xi}. \quad (23)$$

From (22) and (23), one can attain when $t \in (\tau^l_{k+1}, \tau^l_{k+2}]$,

$$V(t) \le \frac{1}{\xi^k} V(t_0)\lambda_{k+1}^{\kappa_{k+1}} \exp((\lambda_A + 6a_1\beta M_1 M_2)(\tau^l_2 - t_0)). \quad (24)$$

Since $V(t_0)\lambda_{k+1}^{\kappa_{k+1}} \exp((\lambda_A + 6a_1\beta M_1 M_2)(\tau^l_2 - t_0))$ is a finite contest, and $1/\xi^k \to 0$ as $k \to \infty$. Thus the synchronization error $e(t)$ can globally asymptotically converges to zero. The proof is completed. □

Remark 1: The consensus condition (13) can be transformed into the following form:

$$\frac{1}{\exp((\lambda_A + 6a_1\beta M_1 M_2)(\tau^l_{k+2} - \tau^l_{k+1}))\lambda_k} > \xi$$

That's to say, the consensus condition is that the constraint combination, which includes system parameters, impulsive control gain, impulsive interval $\tau^l_{k+2} - \tau^l_{k+1}$, is greater than a finite constant $\xi > 1$. Therefore, the constant ξ contributes to the recursive result (24), which shows the existence and necessity of ξ in the consensus condition.

In the proof of Theorem 1, we discuss the interval $t \in (\tau^l_{k+1}, \tau^l_{k+2}]$, $k \in \mathbb{N}$, i.e., the interval between two left endpoints of the adjacent impulsive time windows. If the interval is changed to $t \in (\tau_{k+1}, \tau_{k+2}]$, similarly, i.e., two centers distance of the adjacent impulsive time windows, then we can derive the following Theorem 2.

Theorem 2: Suppose that Assumption 1 hold, if there exists a constant $\xi > 1$ such that

$$(\lambda_A + 6a_1\beta M_1 M_2)(\tau_{k+2} - \tau_{k+1}) + \ln(\lambda_k \xi) < 0, \quad (25)$$

where λ_A and λ_k have same definitions with Theorem 1. Then the synchronization of memristor-based chaotic circuit system (5) and (6) can be realized with controller (7).

Proof: Choose the Lyapunov function as $V(t) = e^T e$, similar to the proof of Theorem 1, i.e., (14)∼(16), for $t \in (t_{k-1}, t_k]$, it yields

$$V(t) \le V((t_{k-1}^+) \exp((\lambda_A + 6a_1\beta M_1 M_2)(t - t_{k-1})). \quad (26)$$

When $V(t_k^+) \le \lambda_k V(t_k)$, similar to Theorem 1, i.e., (17), one can get

$$V(t_k^+) \le \lambda_k V(t_k). \quad (27)$$

For $t \in [t_0, \tau_1]$, there are three cases (see Table 1 and Figs. 3∼5) to be considered.

TABLE 1. The possible case for $t \in [t_0, \tau_1]$.

$t_1 \le \tau_1$	$t \in [t_0, t_1]$	*Case 1*
	$t \in (t_1, \tau_1]$	*Case 2*
$t_1 > \tau_1$	$t \in [t_0, \tau_1]$	*Case 3*

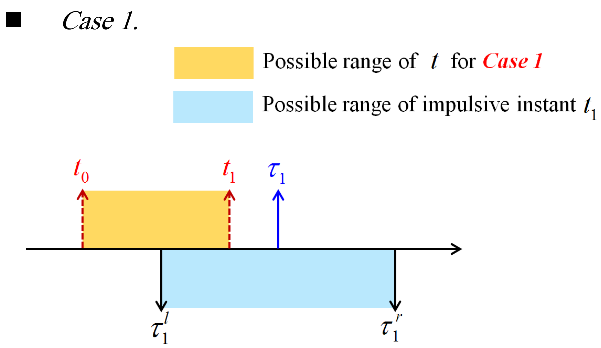

FIGURE 3. The diagram of Case 1 for $t \in [t_0, \tau_1]$.

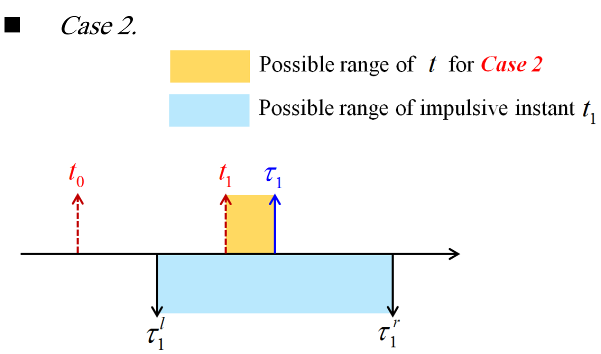

FIGURE 4. The diagram of Case 2 for $t \in [t_0, \tau_1]$.

■ *Case 1:*

It follows from (26) that

$$V(t) \le V(t_0) \exp((\lambda_A + 6a_1\beta M_1 M_2)(t - t_0)). \quad (28)$$

■ *Case 2:*

It follows from (27) and (28)that

$$\begin{aligned} V(t) &\le V(t_1^+) \exp((\lambda_A + 6a_1\beta M_1 M_2)(t - t_1)) \\ &\le \lambda_1 V(t_1) \exp((\lambda_A + 6a_1\beta M_1 M_2)(t - t_1)) \\ &\le \lambda_1 V(t_0) \exp((\lambda_A + 6a_1\beta M_1 M_2)(t_1 - t_0)) \\ &\quad \times \exp((\lambda_A + 6a_1\beta M_1 M_2)(t - t_1)) \\ &= \lambda_1 V(t_0) \exp((\lambda_A + 6a_1\beta M_1 M_2)(t - t_0)). \end{aligned} \quad (29)$$

■ *Case 3:*

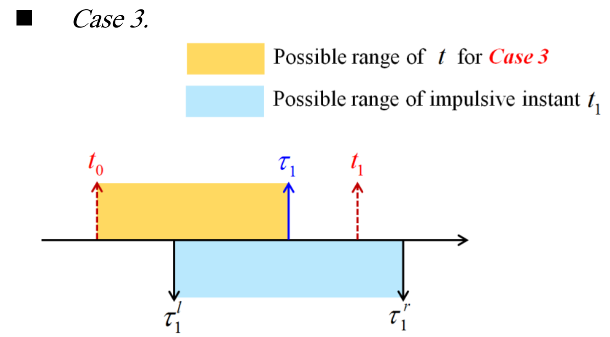

FIGURE 5. The diagram of Case 3 for $t \in [t_0, \tau_1]$.

It follows from (26) that

$$V(t) \le V(t_0) \exp((\lambda_A + 6a_1\beta M_1 M_2)(t - t_0)). \quad (30)$$

Therefore, from (28)∼(30), for $t \in (t_0, \tau_1]$, one can get

$$V(t) \le \lambda_1^{\kappa_1} V(t_0) \exp((\lambda_A + 6a_1\beta M_1 M_2)(t - t_0)), \quad (31)$$

where $\kappa_k (k \in \mathbb{N}_+)$ has the same definition with Theorem 1.

For $t \in (\tau_1, \tau_2]$, there are eight cases (see Table 2 and Figs. 6∼13) to be considered.

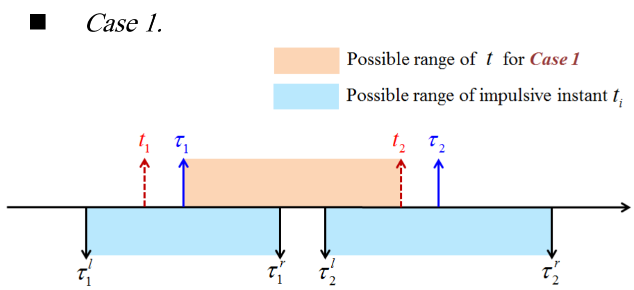

FIGURE 6. The diagram of Case 1 for $t \in (\tau_1, \tau_2]$.

■ *Case 1:*

It follows from (26) and (27) that

$$\begin{aligned} V(t) &\le V(t_1^+) \exp((\lambda_A + 6a_1\beta M_1 M_2)(t - t_1)) \\ &\le \lambda_1 V(t_1) \exp((\lambda_A + 6a_1\beta M_1 M_2)(t - t_1)) \\ &\le \lambda_1 V(t_0) \exp((\lambda_A + 6a_1\beta M_1 M_2)(t_1 - t_0)) \\ &\quad \times \exp((\lambda_A + 6a_1\beta M_1 M_2)(t - t_1)) \\ &= \lambda_1 V(t_0) \exp((\lambda_A + 6a_1\beta M_1 M_2)(t - t_0)). \end{aligned} \quad (32)$$

TABLE 2. The possible case for $t \in [\tau_1, \tau_2]$.

$t_1 \le \tau_1$	$t_2 \le \tau_2$	$t \in (\tau_1, t_2]$	*Case 1*
		$t \in (t_2, \tau_2]$	*Case 2*
	$t_2 > \tau_2$	$t \in (\tau_1, \tau_2]$	*Case 3*
$t_1 > \tau_1$	$t_2 \le \tau_2$	$t \in (\tau_1, t_1]$	*Case 4*
		$t \in (t_1, t_2]$	*Case 5*
		$t \in (t_2, \tau_2]$	*Case 6*
	$t_2 > \tau_2$	$t \in (\tau_1, t_1]$	*Case 7*
		$t \in (t_1, \tau_2]$	*Case 8*

■ *Case 2.*

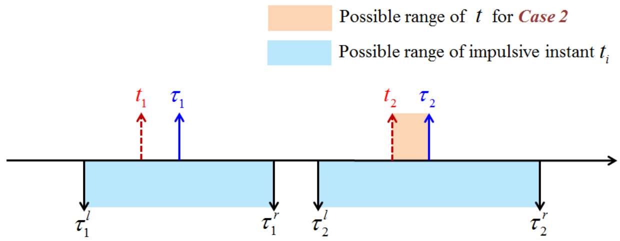

FIGURE 7. The diagram of Case 2 for $t \in (\tau_1, \tau_2]$.

■ *Case 3.*

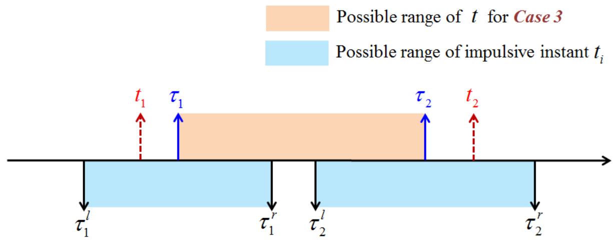

FIGURE 8. The diagram of Case 3 for $t \in (\tau_1, \tau_2]$.

■ *Case 4.*

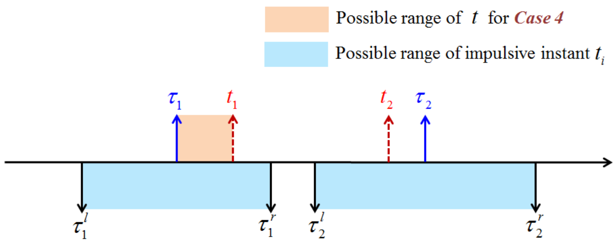

FIGURE 9. The diagram of Case 4 for $t \in (\tau_1, \tau_2]$.

■ *Case 2:*

It follows from (27) and (32) that

$$\begin{aligned} V(t) &\le V(t_2^+)\exp((\lambda_A + 6a_1\beta M_1 M_2)(t - t_2)) \\ &\le \lambda_2 V(t_2)\exp((\lambda_A + 6a_1\beta M_1 M_2)(t - t_2)) \\ &\le \lambda_2\lambda_1 V(t_0)\exp((\lambda_A + 6a_1\beta M_1 M_2)(t_2 - t_0)) \\ &\quad \times \exp((\lambda_A + 6a_1\beta M_1 M_2)(t - t_2)) \\ &= \lambda_1\lambda_2 V(t_0)\exp((\lambda_A + 6a_1\beta M_1 M_2)(t - t_0)). \end{aligned} \tag{33}$$

■ *Case 5.*

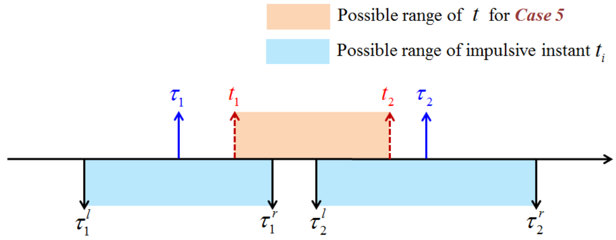

FIGURE 10. The diagram of Case 5 for $t \in (\tau_1, \tau_2]$.

■ *Case 6.*

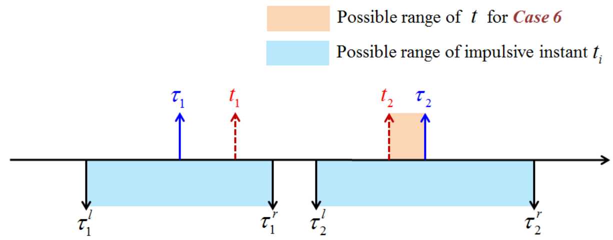

FIGURE 11. The diagram of Case 6 for $t \in (\tau_1, \tau_2]$.

■ *Case 7.*

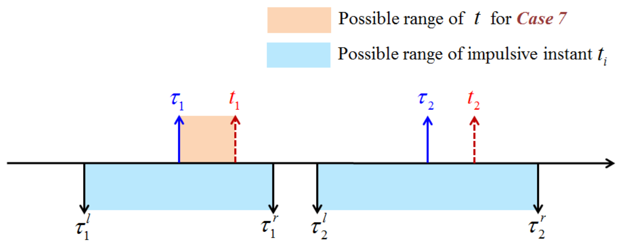

FIGURE 12. The diagram of Case 7 for $t \in (\tau_1, \tau_2]$.

■ *Case 8.*

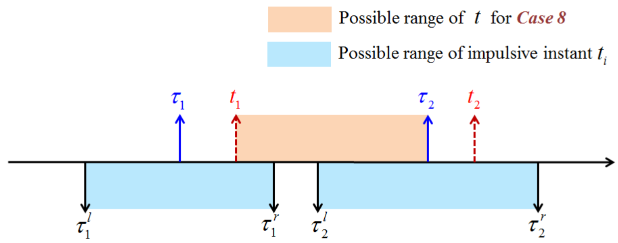

FIGURE 13. The diagram of Case 8 for $t \in (\tau_1, \tau_2]$.

■ *Case 3:*

It follows from (26) and (27) that

$$\begin{aligned} V(t) &\le V(t_1^+)\exp((\lambda_A + 6a_1\beta M_1 M_2)(t - t_1)) \\ &\le \lambda_1 V(t_1)\exp((\lambda_A + 6a_1\beta M_1 M_2)(t - t_1)) \\ &\le \lambda_1 V(t_0)\exp((\lambda_A + 6a_1\beta M_1 M_2)(t_1 - t_0)) \\ &\quad \times \exp((\lambda_A + 6a_1\beta M_1 M_2)(t - t_1)) \\ &= \lambda_1 V(t_0)\exp((\lambda_A + 6a_1\beta M_1 M_2)(t - t_0)). \end{aligned} \tag{34}$$

■ *Case 4:*

It follows from (26) that

$$V(t) \leq V(t_0)\exp((\lambda_A + 6a_1\beta M_1 M_2)(t - t_0)). \quad (35)$$

■ *Case 5:*

It follows from (27) and (35) that

$$\begin{aligned} V(t) &\leq V(t_1^+)\exp((\lambda_A + 6a_1\beta M_1 M_2)(t - t_1)) \\ &\leq \lambda_1 V(t_1)\exp((\lambda_A + 6a_1\beta M_1 M_2)(t - t_1)) \\ &\leq \lambda_1 V(t_0)\exp((\lambda_A + 6a_1\beta M_1 M_2)(t_1 - t_0)) \\ &\quad \times \exp((\lambda_A + 6a_1\beta M_1 M_2)(t - t_1)) \\ &= \lambda_1 V(t_0)\exp((\lambda_A + 6a_1\beta M_1 M_2)(t - t_0)). \end{aligned} \quad (36)$$

■ *Case 6:*

It follows from (27) and (36) that

$$\begin{aligned} V(t) &\leq V(t_2^+)\exp((\lambda_A + 6a_1\beta M_1 M_2)(t - t_2)) \\ &\leq \lambda_2 V(t_2)\exp((\lambda_A + 6a_1\beta M_1 M_2)(t - t_2)) \\ &\leq \lambda_2\lambda_1 V(t_0)\exp((\lambda_A + 6a_1\beta M_1 M_2)(t_2 - t_0)) \\ &\quad \times \exp((\lambda_A + 6a_1\beta M_1 M_2)(t - t_2)) \\ &= \lambda_1\lambda_2 V(t_0)\exp((\lambda_A + 6a_1\beta M_1 M_2)(t - t_0)). \end{aligned} \quad (37)$$

■ *Case 7:*

It follows from (26) that

$$V(t) \leq V(t_0)\exp((\lambda_A + 6a_1\beta M_1 M_2)(t - t_0)). \quad (38)$$

■ *Case 8:*

It follows from (27) and (38) that

$$\begin{aligned} V(t) &\leq V(t_1^+)\exp((\lambda_A + 6a_1\beta M_1 M_2)(t - t_1)) \\ &\leq \lambda_1 V(t_1)\exp((\lambda_A + 6a_1\beta M_1 M_2)(t - t_1)) \\ &\leq \lambda_1 V(t_0)\exp((\lambda_A + 6a_1\beta M_1 M_2)(t_1 - t_0)) \\ &\quad \times \exp((\lambda_A + 6a_1\beta M_1 M_2)(t - t_1)) \\ &= \lambda_1 V(t_0)\exp((\lambda_A + 6a_1\beta M_1 M_2)(t - t_0)). \end{aligned} \quad (39)$$

Based on (32)~(39), for $t \in (\tau_1, \tau_2]$, one can get

$$V(t) \leq \lambda_1^{\kappa_1}\lambda_2^{\kappa_2} V(t_0)\exp((\lambda_A + 6a_1\beta M_1 M_2)(t - t_0)). \quad (40)$$

In general, for $t \in (\tau_{k-1}, \tau_k]$, one can derive

$$\begin{aligned} V(t) \leq\ & V(t_0)\lambda_1\lambda_2\cdots\lambda_{k-2}\lambda_{k-1}^{\kappa_{k-1}}\lambda_k^{\kappa_k} \\ & \times \exp((\lambda_A + 6a_1\beta M_1 M_2)(t - t_0)). \end{aligned} \quad (41)$$

From condition (25), one can get

$$\lambda_k \exp(\lambda_A + 6a_1\beta M_1 M_2)(\tau_{k+2} - \tau_{k+1}) < \frac{1}{\xi}. \quad (42)$$

Therefore, for $t \in (\tau_{k+1}, \tau_{k+2}]$, $k \in \mathbb{N}_+$,

$$\begin{aligned} V(t) &\leq V(t_0)\lambda_1\lambda_2\cdots\lambda_k\lambda_{k+1}^{\kappa_{k-1}}\lambda_{k+2}^{\kappa_k} \\ &\quad \times \exp((\lambda_A + 6a_1\beta M_1 M_2)(t - t_0)) \\ &\leq V(t_0)\lambda_1\lambda_2\cdots\lambda_k\lambda_{k+1}^{\kappa_{k-1}}\lambda_{k+2}^{\kappa_k} \\ &\quad \times \exp((\lambda_A + 6a_1\beta M_1 M_2)(\tau_{k+2} - t_0)) \\ &\leq V(t_0)\exp((\lambda_A + 6a_1\beta M_1 M_2)((\tau_2 - t_0)) \\ &\quad \times \lambda_1\exp((\lambda_A + 6a_1\beta M_1 M_2)(\tau_3 - \tau_2))\cdots \\ &\quad \lambda_k\exp((\lambda_A + 6a_1\beta M_1 M_2)(\tau_{k+2} - \tau_{k+1}))\lambda_{k+1}^{\kappa_{k-1}}\lambda_{k+2}^{\kappa_k} \\ &\leq \frac{1}{\xi^k}V(t_0)\lambda_{k+1}^{\kappa_{k-1}}\lambda_{k+2}^{\kappa_k} \\ &\quad \times \exp((\lambda_A + 6a_1\beta M_1 M_2)(\tau_2 - t_0)). \end{aligned} \quad (43)$$

Since $V(t_0)\lambda_{k+1}^{\kappa_{k-1}}\lambda_{k+2}^{\kappa_k}\exp((\lambda_A + 6a_1\beta M_1 M_2)(\tau_2 - t_0))$ is a finite constant, and $1/\xi^k \to 0$ as $k \to \infty$, Thus the synchronization error $e(t)$ can globally asymptotically converges to zero. The proof is completed. □

Remark 2: Because λ_k is the largest eigenvalue of $(I_n + B_k H(t_k))^T(I_n + B_k H(t_k))$, we can obtain that $\lambda_k \in (0, 1)$ always holds if $b_{ik} \in \Upsilon = (-2, 1) \cup (-1, 0)$ and $h_i(t_k) \in (0, 1]$. One can choose suitable control gain $b_{ik} \in \Upsilon$ to guarantee synchronization goal of the memristor-based chaotic system.

IV. NUMERICAL EXAMPLES

In this section, an example is provided to verify the effectiveness of the main results and illustrate the characteristics of the control method.

Let the parameters be $a_1 = \frac{1}{6.1} * 10^6$, $a_2 = \frac{1}{71} * 10^6$, $a_3 = \frac{1}{2000}$, $a_4 = \frac{1}{15.8} * 10^3$, then one gets

$$A = \begin{bmatrix} 27 & 82 & 0 & 0 \\ 7 & -7 & 14000 & 0 \\ 0 & 63 & 0 & 0 \\ 1 & 0 & 0 & 0 \end{bmatrix}.$$

The estimation of the boundary of the stable region is given by

$$\tau_{k+2}^l - \tau_{k+1}^l < \frac{-\ln(\lambda_k\xi)}{\lambda_A + 6a_1\beta M_1 M_2}, \quad (44)$$

where $M_1 = 200$, $M_2 = 10$.

In this example, we choose the matrix B_k as

$$B_k = \begin{bmatrix} -1.5 & 0 & 0 & 0 \\ 0 & -1.5 & 0 & 0 \\ 0 & 0 & -1.5 & 0 \\ 0 & 0 & 0 & -1.5 \end{bmatrix}.$$

The saturation level is set to $\Delta = 0.25$ in this paper. The initial conditions are given by $x = [0.1253, 0.1302, 0.0924, 0.0078]^T$ and $y = [0.6787, 0.7577, 0.7431, 0.3922]^T$ respectively. The relation between the impulsive instant t_k and left endpoint τ_k^l of k-th impulsive window is shown in Fig.14. Obviously, the actual impulsive instant t_k is greater than the left endpoint instant τ_k^l.

The trajectories in Fig. 15 presents that the synchronization can be realized less than 1.5ms under the proposed impulsive controller, which shows the effectiveness of the proposed variable impulsive control method. With the asymptotic convergence of synchronization error, the control system is no longer affected by the actuator saturation (now matrix $H(t_k)$ become an identity matrix), which is shown in Fig. 16. The impulsive control input is shown in Fig. 17. From Fig. 17, one can see that the size of the impulsive control input will not exceed 0.25 (saturation bound).

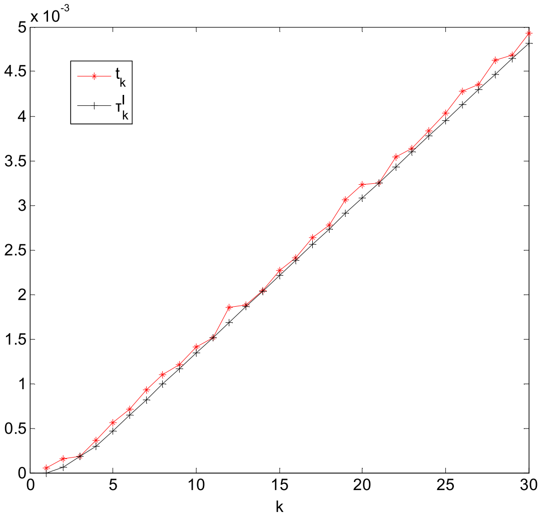

FIGURE 14. The relation between t_k and τ_k^l.

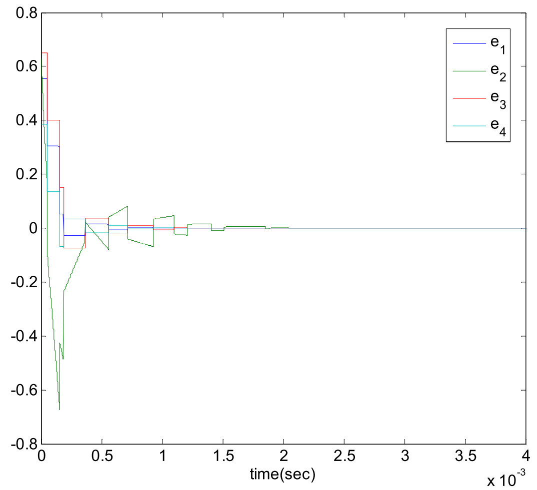

FIGURE 15. Synchronization error for the result in Theorem 1.

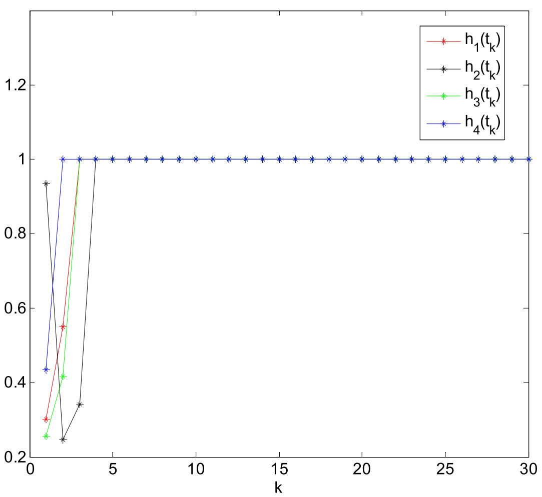

FIGURE 16. The time-varying function $h_i(t_k)$ vs k in Theorem 1.

Now keep B_k, Δ and ξ unchanged, from (25), one can get the center distance of two adjacent impulsive time window as

$$\tau_{k+2} - \tau_{k+1} < \frac{-\ln(\lambda_k \xi)}{\lambda_A + 6a_1\beta M_1 M_2}. \tag{45}$$

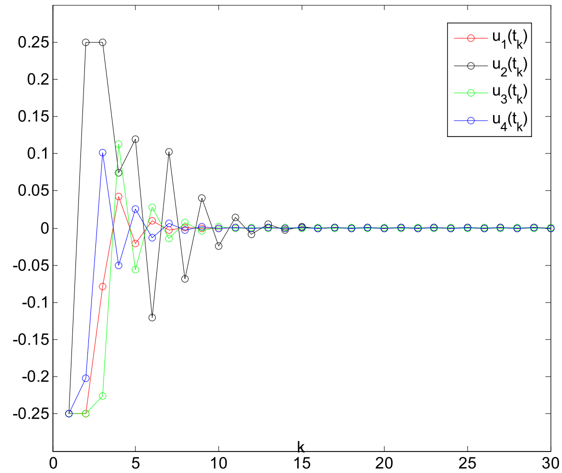

FIGURE 17. The impulsive controller $u(t_k)$ vs k in Theorem 1.

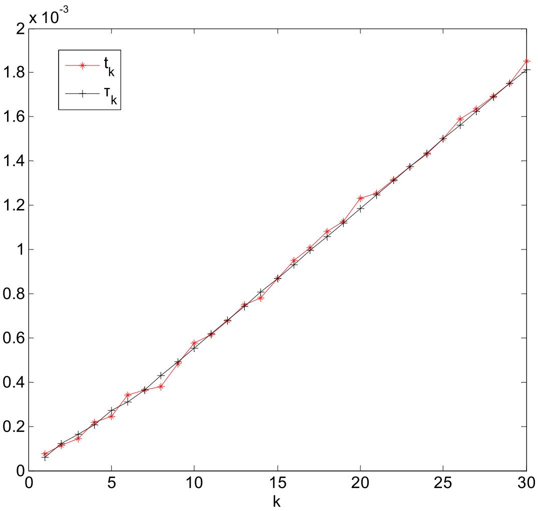

FIGURE 18. The relation between t_k and τ_k.

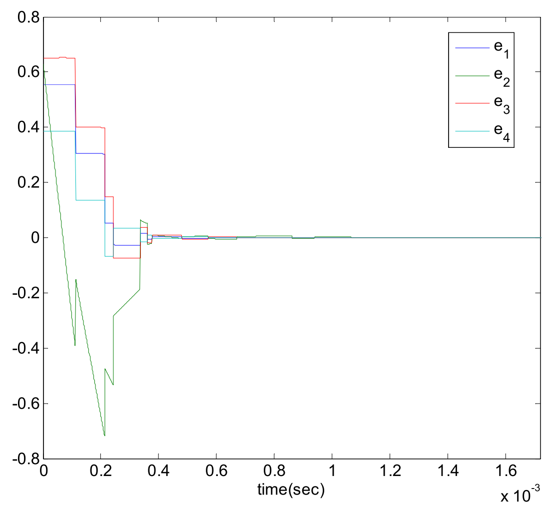

FIGURE 19. Synchronization error for the result in Theorem 2.

The relation between the impulsive instant t_k and the distance between the central points of adjacent impulsive time window τ_k is shown in Fig. 18, which shows that red

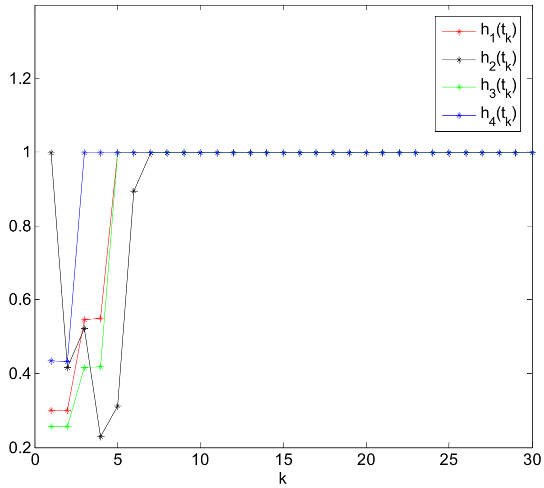

FIGURE 20. The time-varying function $h_i(t_k)$ vs k in Theorem 2.

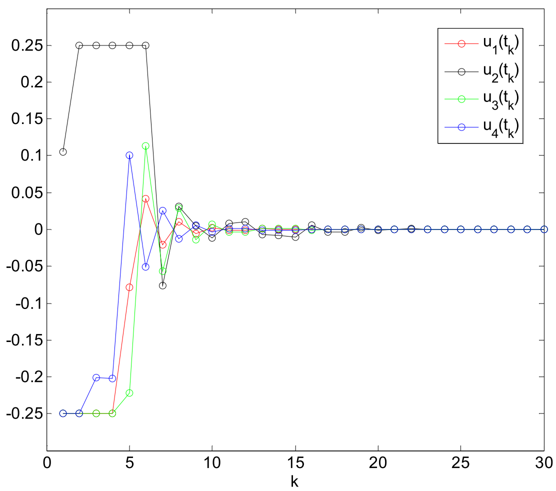

FIGURE 21. The impulsive controller $u(t_k)$ vs k in Theorem 2.

nodes are distributed at both sides of black points (the central points of impulsive time window). Fig. 19 shows that the synchronization of the memristor-based chaotic system can be achieved in 1ms. The corresponding curve of impulsive controller $u(t_k)$ and time-varying function $h_i(t_k)$ are shown in Figs. 20 and 21 respectively.

V. CONCLUSION

This paper studies the variable impulsive synchronization of the memristor-based chaotic system subject to actuator saturation. The controller is provided based on the Lyapunov analysis method. It is worth noting that the impulsive instants are unnecessary to be fixed in this paper. The variable impulsive controller and actuator saturation are considered, which is more reasonable in practical applications. Finally, two simulation examples are given to illustrate the effectiveness of the proposed results. It should be pointed out that future research topics include further promotion and improvement as well as various potential applications, mainly involving the following aspects.

(1) The impulsive synchronization condition in this paper is only a sufficient condition, and it is necessary to further reduce its conservation in our future work.

(2) In practical applications, time delay is inevitable, and how to extend the results in this paper to a more general delay system is an important issue.

(3) For the synchronization problem in real system, the parameters information of systems is usually unknown to the designer. Therefore, adaptive control needs to achieve synchronization when parameters are unknown.

REFERENCES

[1] L. O. Chua, "Memristor—The missing circuit element," *IEEE Trans. Circuit Theory*, vol. CT-18, no. 5, pp. 507–519, Sep. 1971.
[2] D. B. Strukov, G. S. Snider, D. R. Stewart, and R. S. Williams, "The missing memristor found," *Nature*, vol. 453, pp. 80–83, May 2008.
[3] M. Itoh and L. O. Chua, "Memristor oscillators," *Int. J. Bifurcation Chaos*, vol. 18, no. 11, pp. 3183–3206, 2008.
[4] B. Muthuswamy and P. P. Kokate, "Memristor-based chaotic circuits," *IETE Tech. Rev.*, vol. 26, no. 6, pp. 415–426, Nov. 2009.
[5] Q. Xiao, Z. Huang, and Z. Zeng, "Passivity analysis for memristor-based inertial neural networks with discrete and distributed delays," *IEEE Trans. Syst., Man, Cybern. Syst.*, vol. 49, no. 2, pp. 375–385, Feb. 2019.
[6] G. Zhang and Y. Shen, "Exponential stabilization of memristor-based chaotic neural networks with time-varying delays via intermittent control," *IEEE Trans. Neural Netw. Learn. Syst.*, vol. 26, no. 7, pp. 1431–1441, Jul. 2015.
[7] Y. Shi, J. Cao, and G. Chen, "Exponential stability of complex-valued memristor-based neural networks with time-varying delays," *Appl. Math. Comput.*, vol. 313, pp. 222–234, Nov. 2017.
[8] M. Chen, M. Li, Q. Yu, B. Bao, Q. Xu, and J. Wang, "Dynamics of self-excited attractors and hidden attractors in generalized memristor-based Chua's circuit," *Nonlinear Dyn.*, vol. 81, nos. 1–2, pp. 215–226, 2015.
[9] B. Bao, T. Jiang, G. Wang, P. Jin, H. Bao, and M. Chen, "Two-memristor-based Chua's hyperchaotic circuit with plane equilibrium and its extreme multistability," *Nonlinear Dyn.*, vol. 89, no. 2, pp. 1157–1171, 2017.
[10] M. Chen, M. Sun, B. Bao, H. Wu, Q. Xu, and J. Wang, "Controlling extreme multistability of memristor emulator-based dynamical circuit in flux–charge domain," *Nonlinear Dyn.*, vol. 91, pp. 1395–1412, Jan. 2018.
[11] H. Bao, T. Jiang, K. Chu, M. Chen, Q. Xu, and B. Bao, "Memristor-based canonical Chua's Circuit: Extreme multistability in voltage-current domain and its controllability in flux-charge domain," *Complexity*, doi: 10.1155/2018/5935637.
[12] H. Jahanshahi, K. Rajagopal, A. Akgul, N. N. Sari, H. Namazi, and S. Jafari, "Complete analysis and engineering applications of a megastable nonlinear oscillator," *Int. J. Non-Linear Mech.*, vol. 107, pp. 126–136, Dec. 2018.
[13] M. Chen, M. Sun, H. Bao, Y. Hu, and B. Bao, "Flux-charge analysis of two-memristor-based Chua's circuit: Dimensionality decreasing model for detecting extreme multistability," *IEEE Trans. Ind. Electron.*, vol. 67, no. 3, pp. 2197–2206, Mar. 2020.
[14] J. Sun and Y. Shen, "Compound–combination anti-synchronization of five simplest memristor chaotic systems," *Optik*, vol. 127, no. 20, pp. 9192–9200, Oct. 2016.
[15] L. Wang, T. Dong, and M.-F. Ge, "Finite-time synchronization of memristor chaotic systems and its application in image encryption," *Appl. Math. Comput.*, vol. 347, pp. 293–305, Apr. 2019.
[16] Y. Feng, X. Xiong, R. Tang, and X. Yang, "Exponential synchronization of inertial neural networks with mixed delays via quantized pinning control," *Neurocomputing*, vol. 310, pp. 165–171, Oct. 2018.
[17] Y. Feng, X. Yang, Q. Song, and J. Cao, "Synchronization of memristive neural networks with mixed delays via quantized intermittent control," *Appl. Math. Comput.*, vol. 339, no. 15, pp. 874–887, Dec. 2018.
[18] H. Jahanshahi, A. Yousefpour, Z. Wei, R. Alcaraz, and S. Bekiros, "A financial hyperchaotic system with coexisting attractors: Dynamic investigation, entropy analysis, control and synchronization," *Chaos, Solitons Fractals*, vol. 126, pp. 66–77, Sep. 2019.
[19] Z. Yang, B. Luo, D. Liu, and Y. Li, "Pinning synchronization of memristor-based neural networks with time-varying delays," *Neural Netw.*, vol. 93, pp. 143–151, Sep. 2017.

[20] J. Liu and X. Rui, "Adaptive synchronisation of memristor-based neural networks with leakage delays and applications in chaotic masking secure communication," *Int. J. Syst. Sci.*, vol. 49, no. 6, pp. 1–16, Mar. 2018.
[21] G. Min, S. Duan, and L. Wang, "A double-wing chaotic system based on ion migration memristor and its sliding mode control," *Int. J. Bifurcation Chaos*, vol. 26, no. 8, 2016, Art. no. 1650129.
[22] A. Wu, S. Wen, and Z. Zeng, "Synchronization control of a class of memristor-based recurrent neural networks," *Inf. Sci.*, vol. 183, no. 1, pp. 106–116, 2012.
[23] T. Ma and J. Fu, "On the exponential synchronization of stochastic impulsive chaotic delayed neural networks," *Neurocomputing*, vol. 74, no. 5, pp. 857–862, Feb. 2011.
[24] Y. Wang, W. Yang, J. Xiao, and Z. Zeng, "Impulsive multi-synchronization of coupled multistable neural networks with time-varying delay," *IEEE Trans. Neural Netw. Learn. Syst.*, vol. 28, no. 7, pp. 1560–1571, Jul. 2017.
[25] Y. Li, "Impulsive synchronization of stochastic neural networks via controlling partial states," *Neural Process. Lett.*, vol. 46, no. 1, pp. 59–69, 2017.
[26] B. Xiao, Q. Hu, and Y. Zhang, "Adaptive sliding mode fault tolerant attitude tracking control for flexible spacecraft under actuator saturation," *IEEE Trans. Control Syst. Technol.*, vol. 20, no. 6, pp. 1605–1612, Nov. 2012.
[27] L. Fu and Y. Ma, "Dissipative control for singular time-delay system with actuator saturation via state feedback and output feedback," *Int. J. Syst. Sci.*, vol. 49, no. 3, pp. 639–652, Mar. 2017.
[28] H. Shao and J. Zhao, "Control and optimization of sampled-data systems with quantization and actuator Saturation," *J. Syst. Sci. Complex.*, vol. 30, no. 6, pp. 1242–1257, Dec. 2017.
[29] J. Wei, Y. Zhang, M. Sun, and B. L. Geng, "Adaptive neural synchronization control of chaotic systems with unknown control directions under input saturation," *Optik-Int. J. Light Electron Opt.*, vol. 132, pp. 249–261, Mar. 2017.
[30] A. H. Tahoun, "Anti-windup adaptive PID control design for a class of uncertain chaotic systems with input saturation," *ISA Trans.*, vol. 66, pp. 176–184, Jan. 2017.
[31] S. Shao, M. Chen, and X. Yan, "Prescribed performance synchronization for uncertain chaotic systems with input saturation based on neural networks," *Neural Comput. Appl.*, vol. 29, no. 12, pp. 1349–1361, Jun. 2018.
[32] X. Zhang and H. Wu, "H_∞ control design for memristor-based neural networks subject to actuator saturation," in *Proc. 36th Chin. Control Conf.*, Jul. 2017, pp. 4000–4005.
[33] B. Zhang, F. Deng, S. Xie, and S. Luo, "Exponential synchronization of stochastic time-delayed memristor-based neural networks via distributed impulsive control," *Neurocomputing*, vol. 286, no. 19, pp. 41–50, Apr. 2018.
[34] J. Fu, J. F. Bai, J. J. Lai, P. D. Li, M. Yu, and H. K. Lam, "Adaptive fuzzy control of a magnetorheological elastomer vibration isolation system with time-varying sinusoidal excitations," *J. Sound Vib.*, vol. 456, pp. 386–406, Jun. 2016.
[35] Q. Fu, T. Cai, S. Zhong, and Y. Yu, "Pinning impulsive synchronization of stochastic memristor-based neural networks with time-varying delays," *Int. J. Control, Autom. Syst.*, vol. 17, no. 1, pp. 243–252, Jan. 2019.
[36] W. Xiong and J. Huang, "Finite-time control and synchronization for memristor-based chaotic system via impulsive adaptive strategy," *Adv. Difference Equ.*, to be published, doi: 10.1186/s13662-016-0789-3.
[37] X. Wang, H. Wang, C. Li, and T. Huang, "Synchronization of coupled delayed switched neural networks with impulsive time window," *Nonlinear Dyn.*, vol. 84, no. 3, pp. 1747–1757, Feb. 2016.
[38] T. Ma, Z. Zhang, and B. Cui, "Variable impulsive consensus of nonlinear multi-agent systems," *Nonlinear Anal., Hybrid Syst.*, vol. 31, pp. 1–18, Feb. 2019.
[39] T. Ma, T. Yu, and B. Cui, "Adaptive synchronization of multi-agent systems via variable impulsive control," *J. Franklin Inst.*, vol. 355, no. 15, pp. 7490–7508, Oct. 2018.
[40] X. Wang, J. Yu, C. Li, H. Wang, T. Huang, and J. Huang, "Robust stability of stochastic fuzzy delayed neural networks with impulsive time window," *Neural Netw.*, vol. 67, pp. 84–91, Jul. 2015.
[41] Y. Feng, C. Li, and T. Huang, "Sandwich control systems with impulse time windows," *Int. J. Mach. Learn. Cybern.*, vol. 8, no. 6, pp. 2009–2015, Dec. 2017.
[42] X. Hu and L. Nie, "A note on sandwich control systems with impulse time windows," *Medit. J. Math.*, to be published, doi: 10.1007/s00009-019-1310-5.
[43] J. Tan, C. Li, and T. Huang, "Comparison system method for a class of stochastic systems with variable-time impulses," *Int. J. Control, Autom. Syst.*, vol. 16, no. 2, pp. 702–708, Apr. 2018.
[44] Y. Feng, C. Li, and T. Huang, "Periodically multiple state-jumps impulsive control systems with impulse time windows," *Neurocomputing*, vol. 193, no. 12, pp. 7–13, Jun. 2016.
[45] P. Wu, C. D. Li, X. He, and T. Huang, "A memristor-based Lorenz circuit and its stabilization via variable-time impulsive control," *Int. J. Bifurcation Chaos*, vol. 27, no. 3, 2017, Art. no. 1750031.
[46] F. L. Chen, H. Wang, and C. Li, "Impulsive control of memristive chaotic systems with impulsive time window," *Math. Problems Eng.*, vol. 2015, Mar. 2015, Art. no. 727937.
[47] B. Muthuswamy, "Implementing memristor based chaotic circuits," *Int. J. Bifurcation Chaos*, vol. 20, no. 5, pp. 1335–1350, May 2010.
[48] M. Chen, B. Bao, T. Jiang, H. Bao, Q. Xu, H. Wu, and J. Wang, "Flux-charge analysis of initial state-dependent dynamical behaviors of a memristor emulator-based Chua's circuit," *Int. J. Bifurcation Chaos*, vol. 28, no. 10, 2018, Art. no. 1850120, doi: 10.1142/S0218127418501201.
[49] Y. N. Joglekar and S. J. Wolf, "The elusive memristor: Properties of basic electrical circuits," *Eur. J. Phys.*, vol. 30, no. 4, pp. 661–675, May 2009.

ZHILI XIONG received the M.S. degree in control theory and control engineering from Northeast University, Shenyang, China, in 2007. He is currently pursuing the Ph.D. degree with the Department of Electronics and Information Engineering, Central China Normal University, Wuhan, China. His research interests include intelligent information processing and control, chaos synchronization of memristor, and impulsive control.

ZHENGLE ZHANG was born in Henan, China, in 1995. He received the B.S. degree from the School of Automation, Chongqing University, Chongqing, China, in 2017. He is currently pursuing the Ph.D. degree with the School of Automation, Chongqing University. His main research interests include cooperative control of multiagent systems and impulsive control.

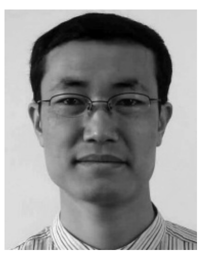

TIEDONG MA was born in Liaoning, China, in 1978. He received the Ph.D. degree in control theory and control engineering from Northeastern University, Shenyang, China, in 2009. He is currently an Associate Professor with the School of Automation, Chongqing University, Chongqing, China. His main research interests are cooperative control of multiagent systems, as well as impulsive control and synchronization of complex networks.